Sakashita *et al. Geosci. Lett. (2017) 4:29*
https://doi.org/10.1186/s40562-017-0095-2

Geoscience Letters

RESEARCH LETTER

Open Access

Relationship between the Northern Pacific Gyre Oscillation and tree-ring cellulose oxygen isotopes in northeastern Japan

Wataru Sakashita[1,2,3*], Hiroko Miyahara[1], Yusuke Yokoyama[3,4,5], Takahiro Aze[3], Stephen P. Obrochta[6] and Takeshi Nakatsuka[7]

Abstract
The North Pacific Gyre Oscillation (NPGO) significantly imprints on hydrological fluctuations of the East Asian summer monsoon (EASM) region, but this has not yet been observed in proxy-based hydroclimate reconstructions. This study reports a tree-ring cellulose oxygen isotope ($\delta^{18}O$) record from northeastern Japan spanning A.D. 1927–2010, overlapping with instrumental data, which we analyzed to determine if tree-ring $\delta^{18}O$ in northeastern Japan records a signal consistent with the NPGO. Our results indicate that the tree-ring $\delta^{18}O$ has a significant negative correlation with May–June (MJ) precipitation, as well as with short-term MJ relative humidity variation. Time-lagged temporal-domain comparisons indicate that the tree-ring $\delta^{18}O$ is significantly correlated with the following year March–April (MA) and MJ NPGO index before the North Pacific climate transition in the late 1980s, particularly on decadal timescales. These relationships between our tree-ring $\delta^{18}O$ and the climate patterns in the North Pacific are consistent with the actual early-summer precipitation. Spatial spring and early-summer sea-surface temperature anomalies exhibit a NPGO-like pattern in the following year. Spatial early-summer sea-level pressure anomalies also indicate North Pacific Oscillation (NPO) like patterns in the western North Pacific. These results suggest a lagged response of the NPGO to the EASM climate changes, and tree-ring $\delta^{18}O$ in northeast Japan has a potential linkage with NPGO index from winter to early summer of the following year.

Keywords: Tree-ring, Oxygen isotope, Northeastern Japan, North Pacific Gyre Oscillation, North Pacific Oscillation

Background

Decadal climate changes in the Pacific Ocean are an important issue because these fluctuations may affect the rate of surface warming through increased subsurface ocean heat uptake (e.g., England et al. 2014) and cause changes in marine ecosystems (e.g., Mantua et al. 1997). Sea-surface temperature (SST) patterns in the North Pacific region are characterized by the Pacific Decadal Oscillation (PDO; Mantua et al. 1997; Zhang et al. 1997) and the North Pacific Gyre Oscillation (NPGO; Di Lorenzo et al. 2008). The PDO is the first leading empirical orthogonal function (EOF) mode of SST anomalies (Mantua et al. 1997; Zhang et al. 1997), and the NPGO is defined as the second leading EOF mode of the sea-surface height (SSH) anomalies (Di Lorenzo et al. 2008). The SSH pattern of the NPGO is also consistent with the second EOF mode of the SST anomalies (Bond and Harrison 2000) which are forced by dipole sea-level pressure (SLP) anomalies in the North Pacific (Di Lorenzo et al. 2008), the so-called North Pacific Oscillation (NPO; Rogers 1981).

Recently, a number of studies indicate that the impact of NPGO on the climate system is increasing due to an amplification in the late 1980s, which is similar in amplitude to that of the PDO (Yeh et al. 2011). Previous work reported that the NPGO synchronizes the climate variability in the western North Pacific boundary [Kuroshio–Oyashio Extension (KOE) region] with a lag of 2–3 years, and the westward propagating Rossby wave is responsible

*Correspondence: sakashita.wataru.fu@u.tsukuba.ac.jp
[1] Humanities and Sciences, Musashino Art University, 1-736 Ogawa-cho, Kodaira, Tokyo 187-8505, Japan
Full list of author information is available at the end of the article

for this variation (Ceballos et al. 2009). Previous studies also examined the relationship between the NPGO and western boundary of the North Pacific summer climate system (Zhang and Luo 2016; Ye et al. 2016). The western North Pacific summer monsoon (WNPSM) has a significant impact on the NPGO in March–April–May of the following year (Zhang and Luo 2016), and the NPGO also appears to influence the East Asian summer precipitation (Ye et al. 2016).

To develop understanding of the long-term fluctuation in the North Pacific Ocean, proxy-based paleoclimate reconstructions are necessary because instrumental records are sufficient for calculating the PDO index (Mantua et al. 1997; Zhang et al. 1997) and the NPGO (Di Lorenzo et al. 2008) index from only A.D. 1900 and A.D. 1950, respectively. While previous studies have reported PDO reconstructions using various climate proxies (e.g., tree-ring width, historical documents, coral) (D'Arrigo and Wilson 2006; Shen et al. 2006; Felis et al. 2010), NPGO reconstruction (performed using hydrogen isotopes of the ice core in the central Kamchatka) only shows significant correlation to the NPGO index following a climate regime shift in A.D. 1976/1977 (Sato et al. 2014). In the central tropical Pacific (Palmyra Island), a coral Sr/Ca-based SST record is highly correlated to the NPGO index on decadal timescales over the twentieth century (Nurhati et al. 2011) due to the NPGO relationship with the central Pacific El Niño (Di Lorenzo et al. 2010). Recently, coral radiocarbon data from the eastern tropical North Pacific (San Benedicto Island) show that this variability reflects NPGO-driven gyre circulation and regional coastal upwelling (Rafter et al. 2017). However, there is yet no NPGO reconstruction in the western boundary region of the North Pacific. Hydroclimate reconstruction from the northern limit of the East Asian summer monsoon may produce NPGO proxy, increasing our understanding of its dynamics over the recent centuries.

Thus, we examine the feasibility of constructing an NPGO proxy based on tree-ring cellulose oxygen isotopes (δ^{18}O) that reflects relative humidity by means of the tree from northeastern Japan. In general, mid-latitude atmospheric water vapor is sourced from tropical regions, with relatively stable oxygen isotopes ratios in the western tropical Pacific (e.g., Yokoyama et al. 2011). Because summer rainfall δ^{18}O at mid latitudes is negatively correlated to precipitation amount (amount effect; Dansgaard 1964), and this precipitation generally has positive correlation with the relative humidity in Japan, we are able to reconstruct early-summer hydrological conditions in central Japan using the tree-ring δ^{18}O (e.g., Yamaguchi et al. 2010; Li et al. 2015; Sakashita et al. 2016, 2017).

Here, we report a new tree-ring cellulose δ^{18}O record for northeastern Japan spanning A.D. 1927–2010. This interval overlaps with the instrumental records of the nearest meteorological station. Comparisons of our dataset with the instrumental NPGO index allow us to consider whether tree-ring δ^{18}O in northeastern Japan can be a proxy for the NPGO index.

Methods

Tree-ring cellulose δ^{18}O theory

Theoretically, the leaf δ^{18}O model is expressed as the following modified Craig–Gordon equation (Craig and Gordon 1965):

$$\delta^{18}\mathrm{O}_{\mathrm{leaf}} = \delta^{18}\mathrm{O}_x + \varepsilon^* + \varepsilon_k + e_a/e_i\left(\delta^{18}\mathrm{O}_a - e_k - \delta^{18}\mathrm{O}_x\right), \tag{1}$$

where $\delta^{18}\mathrm{O}_{\mathrm{leaf}}$ indicates the oxygen isotopes in leaves, and e_a (e_i) refers to the ambient vapor pressure (vapor pressure inside the leaves). $\delta^{18}\mathrm{O}_a$ ($\delta^{18}\mathrm{O}_x$) is the oxygen isotope ratios of atmospheric vapor (stem water), and ε^* (ε_k) indicates the equilibrium (kinetic) isotope fractionation factor. Previous studies regard $\delta^{18}\mathrm{O}_x$ (e_a/e_i) as the oxygen isotope of precipitation (relative humidity) on some hypotheses, and this equation [Eq. (1)] is expressed as the following equation (e.g., Xu et al. 2011; Sano et al. 2012):

$$\delta^{18}\mathrm{O}_{\mathrm{leaf}} = \delta^{18}\mathrm{O}_p + \left(\varepsilon^* + \varepsilon_k\right)(1-h), \tag{2}$$

where $\delta^{18}\mathrm{O}_p$ and h indicate the oxygen isotopes of precipitation and relative humidity, respectively. Considering the biochemical fractionation in sucrose synthesis, previous studies (Roden et al. 2000; Sternberg 2009) calculate cellulose oxygen isotopes ($\delta^{18}\mathrm{O}_c$) as follows:

$$\delta^{18}\mathrm{O}_c = f\left(\delta^{18}\mathrm{O}_x + \varepsilon_0\right) + (1-f)\left(\delta^{18}\mathrm{O}_{\mathrm{leaf}} + 27‰\right) \tag{3}$$

In Eq. (3), f is the ratio of oxygen that exchanges with xylem water, and ε_0 indicates the isotopic fractionation factor between exchanged oxygen from carbohydrate and xylem water during cellulose synthesis. Previous results examine the negligibly small influence of biochemical fractionation in this equation. Thus, cellulose δ^{18}O is theoretically controlled by the oxygen isotopes of precipitation and relative humidity (Roden et al. 2000; McCarroll and Loader 2004; Sternberg 2009; Managave et al. 2010).

Tree-ring cellulose δ^{18}O measurement

We measured tree-ring cellulose δ^{18}O in northeast Japan from A.D. 1927–2010 to examine the climate response of our data to the closest meteorological station (Sendai; Fig. 1), records from which extend from October 1926 to present. Our sample was acquired at Kashima shrine

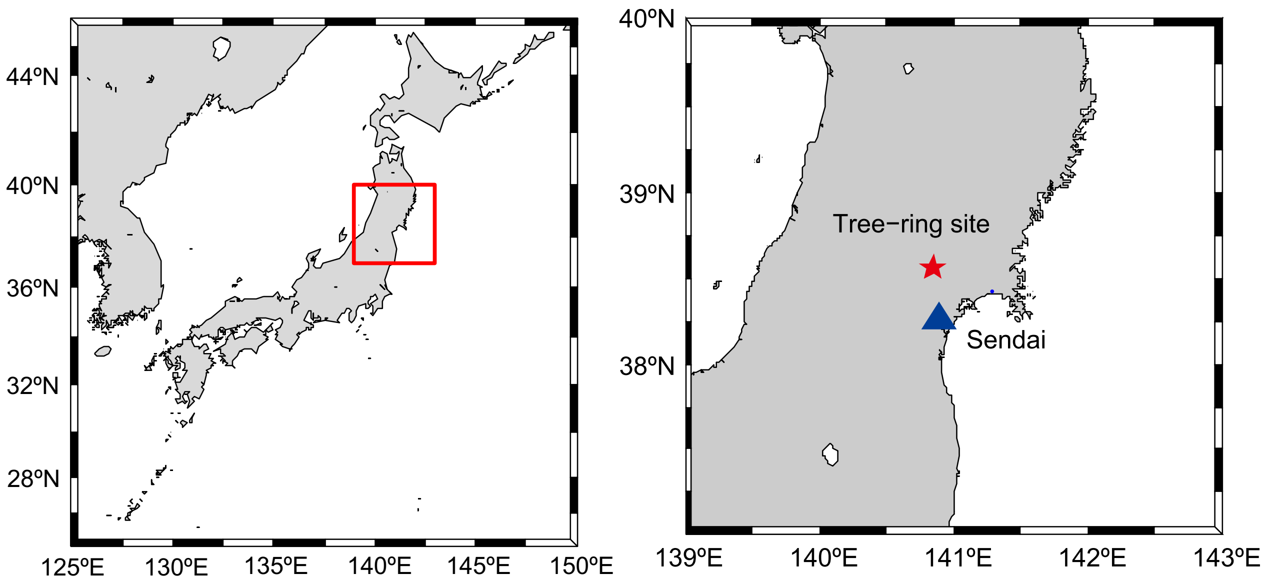

Fig. 1 Map of northeast Japan showing the tree-ring sample site and meteorological station (Sendai). Red star indicates the tree-ring site, and blue triangle shows Sendai

in Miyagi prefecture (38°33′N, 140°52′E; Fig. 1) in A.D. 2010. Application of the "plate method" (Xu et al. 2011; Kagawa et al. 2015) enabled us to obtain an extracted α-cellulose plate from our sample, which is then divided into annual growth rings. Growth rings (0.2 mg) were individually wrapped in silver foil, with $\delta^{18}O$ measured at least twice for each sample using both a continuous flow high-temperature conversion elemental analyzer (TC/EA), as well as a Thermo Finnigan MAT253 mass spectrometer at the Tokyo Institute of Technology (Sakashita et al. 2016). Repeated analyses of the working standard (Merck cellulose) showed that measurement uncertainties are less than 0.3‰. Resulting oxygen isotope ratios are expressed in the following standard equation:

$$\delta^{18}O = \left(\left({}^{18}O/{}^{16}O\right)_{sample} \Big/ \left({}^{18}O/{}^{16}O\right)_{standard} - 1\right) \times 1000‰,$$

where the oxygen standard is Vienna Standard Mean Ocean Water (VSMOW).

Meteorological data and spectral analysis

Meteorological data (temperature, precipitation, and relative humidity) from the Sendai station (38°16′N, 140°54′E; Fig. 1) enabled us to examine the climate response of our tree-ring $\delta^{18}O$ data. These data are available from the Japan Meteorological Agency [http://www.data.jma.go.jp/obd/stats/etrn/index.php (Japanese-language site)].

We also compare $\delta^{18}O$ of tree-ring cellulose to the NPGO index from A.D. 1950 to 2010 (Di Lorenzo et al. 2008), which is available at http://www.o3d.org/npgo/npgo.php and to the PDO index (Mantua et al. 1997; Zhang et al. 1997) (data available from http://research.jisao.washington.edu/pdo/). Here we excluded the years of A.D. 2010 through 2016 from these analyses, because our tree-ring sample recorded until A.D. 2010. We also use global SST and SLP datasets from A.D. 1927 to 2010. SST data were obtained from the Extended Reconstructed SST version 3b [ERSST v3b; Smith et al. (2008)] dataset of the National Oceanic and Atmospheric Administration (NOAA) (available from https://www.ncdc.noaa.gov/data-access/marineocean-data/extended-reconstructed-sea-surface-temperature-ersst-v3b). SLP data were obtained from the National Centers for Environmental Prediction (NCEP) and the National Center for Atmospheric Research (NCAR) reanalysis 1 (Kalnay et al. 1996; available from http://www.esrl.noaa.gov/psd/data/gridded/data.ncep.reanalysis.surface.html). We also use both the 20th century Reanalysis (V2) of NOAA Earth System Research Laboratory (ESRL) (Compo et al. 2011) and the European Centre for Medium-Range Weather Forecasts (ECMWF) 20th century reanalysis (ERA-20C) (Poli et al. 2016).

To examine periodicity, we applied multitaper method (MTM) analysis using the software package kSpectra (Ghil 2002). In this analysis, the significance test was based on an AR (1) (red) null hypothesis. Wavelet code was used to examine the coherency in time–frequency space (Grinsted et al. 2004).

Results and discussion

Climate response of tree-ring cellulose $\delta^{18}O$

Comparisons between tree-ring $\delta^{18}O$ and precipitation recorded from the Sendai station reveal that the highest significant correlation is to May–June (MJ) precipitation ($r = -0.37$, $p < 0.001$, $N = 84$) (Fig. 2a). Significant correlations also exist with precipitation during May ($r = -0.28$, $p < 0.05$, $N = 84$), June ($r = -0.25$, $p < 0.05$, $N = 84$), April–May–June ($r = -0.29$, $p < 0.01$, $N = 84$), May–June–July ($r = -0.28$, $p < 0.01$, $N = 84$), February–March–April–May ($r = -0.26$, $p < 0.05$, $N = 84$), March–April–May–June ($r = -0.31$, $p < 0.01$, $N = 84$), and April–May–June–July ($r = -0.26$, $p < 0.05$, $N = 84$) (Additional file 1: Figure S1a–c). Comparisons between our data and relative humidity showed that the highest correlation was found for the MJ relative humidity ($r = -0.20$, $p < 0.1$, $N = 84$) (Fig. 2b; Additional file 1: Figure S1d–f). In the comparison with temperature, the highest correlation occurred at May temperature ($r = 0.20$, $p < 0.1$, $N = 84$) (Fig. 2c; Additional file 1: Figure S1g–i). However, neither of these correlations are significant in the 95% confidence level. Figure 3 shows the comparison between our tree-ring $\delta^{18}O$ data and MJ meteorological data (precipitation and relative humidity) from A.D. 1927 to 2010, indicating that tree-ring $\delta^{18}O$ in northeast Japan was influenced by early-summer precipitation variability (Fig. 3a, d).

Temporal comparison with MJ relative humidity also indicates that the tree-ring data do not record long-term relative humidity variations (Fig. 3b, e). MTM analyses of both tree-ring $\delta^{18}O$ and MJ precipitation during A.D. 1927–2010 reveal no significant spectral peaks (Fig. 4a, c), but same analysis for MJ relative humidity showed a significant long-term variation (gray shade in Fig. 4b). To compare our tree-ring data with MJ relative humidity except for this variation, we removed the lower-frequency component from both datasets with 57-year high-pass filter. After removal, correlation analysis between these $\delta^{18}O$ and MJ relative humidity datasets exhibit a significant correlation ($r = -0.37$, $p < 0.001$, $N = 84$; Fig. 3c, f). Thus, our tree-ring $\delta^{18}O$ are influenced by both early-summer precipitation and short-term relative humidity variation.

Comparison with NPGO, PDO and SST

To examine the relationship between tree-ring $\delta^{18}O$ in northeast Japan and North Pacific SST, we compared our data to the NPGO (Di Lorenzo et al. 2008) and PDO (Zhang et al. 1997) indices from A.D. 1950 to 2010. Seasonal time-lagged correlation analyses reveal significant correlation exists for the following year January–February (+JF) NPGO index ($r = 0.28$, $p < 0.05$, $N = 61$) and following year MJ (+MJ) NPGO index ($r = 0.26$, $p < 0.05$, $N = 61$) (Table 1). These analyses also show that there is no significant correlation between tree-ring $\delta^{18}O$ in northeast Japan and PDO index (Table 1). We also investigated yearly time-lagged relationships between our record and the NPGO index. Previous work reported that the NPGO synchronizes the climate variability in the western North Pacific boundary with a lag of 2–3 years (Ceballos et al. 2009). However, we find no significant correlation between our tree-ring $\delta^{18}O$ and the MJ NPGO index with a lag of about 3 years ($r = 0.01$, $p > 0.10$ for 2-year lag; $r = -0.15$, $p > 0.10$ for 3-year lag; $r = -0.07$, $p > 0.10$ for 4-year lag).

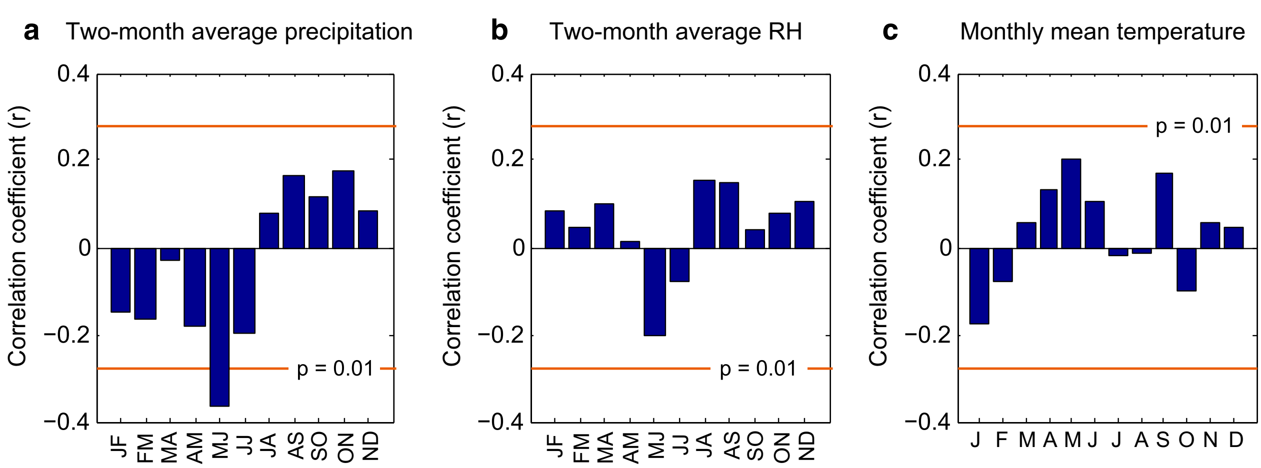

Fig. 2 Correlation between tree-ring $\delta^{18}O$ and **a** 2-month average precipitation, **b** 2-month average relative humidity (RH), **c** monthly mean temperature in Sendai. Red lines indicate the significant level 99%. *J* January, *F* February, *M* March, *A* April, *M* May, *J* June, *J* July, *A* August, *S* September, *O* October, *N* November, *D* December

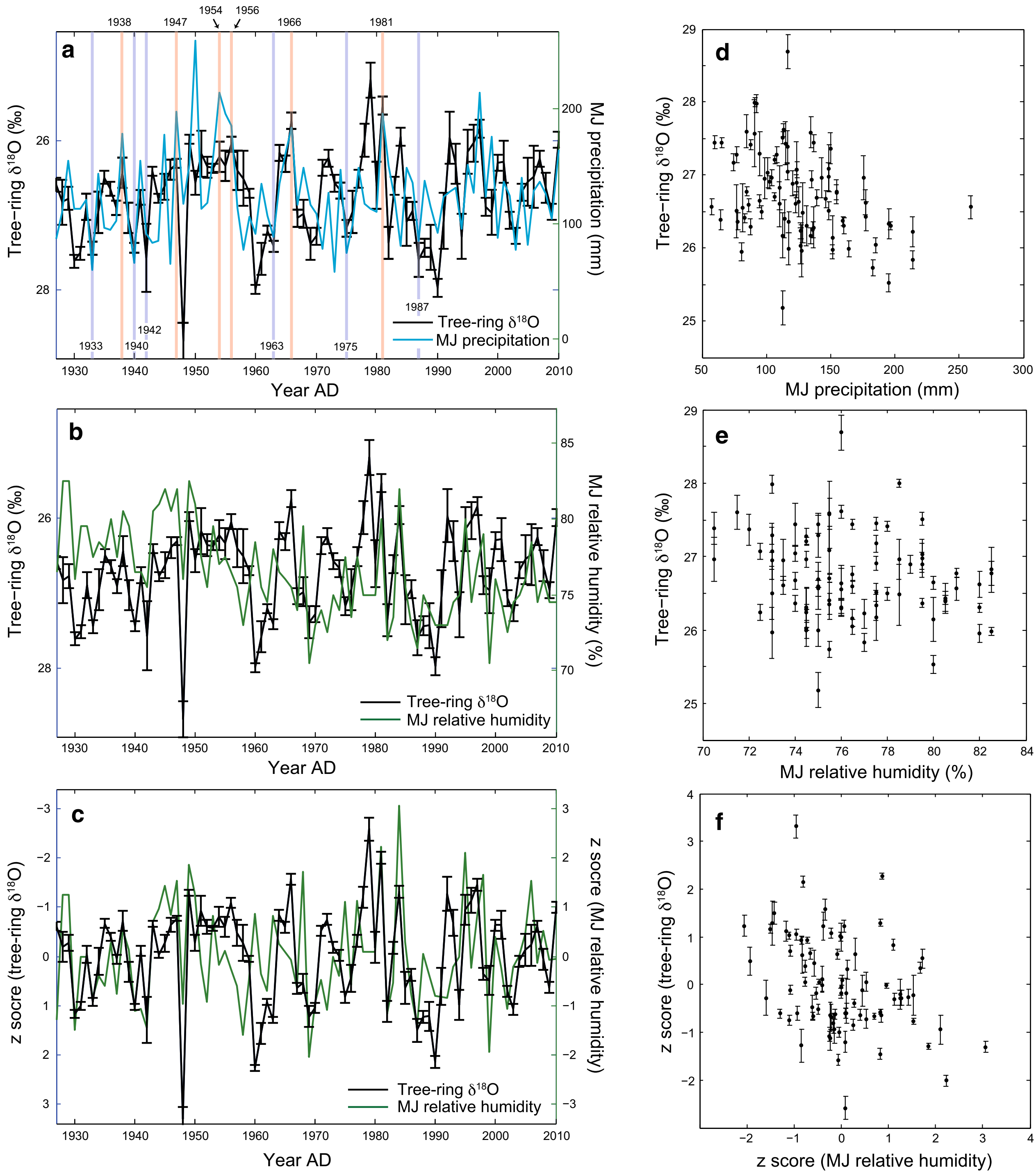

Fig. 3 Temporal comparisons between tree-ring $\delta^{18}O$ and **a** MJ precipitation, and **b** MJ relative humidity in Sendai station from A.D. 1927 to 2010. **c** Tree-ring $\delta^{18}O$ and MJ relative humidity after removal of low-frequency component. Black, blue, and green solid lines indicate tree-ring $\delta^{18}O$, MJ precipitation, and MJ relative humidity, respectively. *Z*-score is zero mean and unit standard deviation. Scatter plot of tree-ring $\delta^{18}O$ versus **d** MJ precipitation, and **e** MJ relative humidity. **f** Scatter plot of tree-ring $\delta^{18}O$ versus MJ relative humidity after removal of low-frequency component

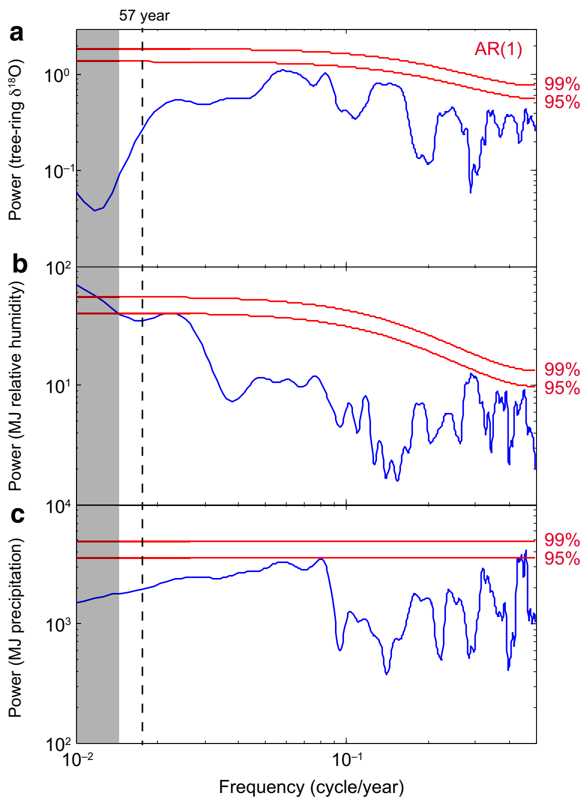

Fig. 4 Results of MTM analysis for **a** tree-ring δ^{18}O, **b** MJ relative humidity, and **c** MJ precipitation in Sendai station. Analysis period is from A.D. 1927 to 2010. Red solid lines indicate 95 and 99% significant level, and black dot line corresponds to 57-year cycle

We also performed decadal time scale comparisons between tree-ring δ^{18}O in northeast Japan and the NPGO index to confirm the results of a previous study indicating that the NPGO is characterized by decadal variations (e.g., Di Lorenzo et al. 2008, 2010). MTM analyses of both the tree-ring δ^{18}O and NPGO index [+JF, following year March–April (+MA), +MJ] were performed from A.D. 1950 to 2010. These results suggested similar spectral peaks indicating a 3- to 30-year cycle (Additional file 2: Figure S2), though other significant spectral frequencies are evident during this period. We also performed the cross-wavelet analyses for our tree-ring δ^{18}O and the NPGO indices to understand the coherency in time–frequency space. These analyses indicate common variance on both multiyear and decadal time scales, but the coherence at periods of 5–10 years only appeared during the 1970s and 1980s (Additional file 3: Figure S3). Further studies are needed to explain why these correlations were only found during these periods. To extract these common components of both our data and NPGO index, we applied two band-pass filters, centered at 0.1 year^{-1} with 3–30- and 5–30-year bandwidth (Fig. 5). Correlation analyses revealed that 5–30-year variability of tree-ring δ^{18}O had the highest correlations with that of +MJ NPGO index from A.D. 1950 to 2010, but this correlation coefficient was not significant in 95% level using estimates of the effective number of degree of freedom ($r = 0.44$, d$f = 15$, $p = 0.1$; Table 2). We also investigated this decadal relationship at the different time intervals (A.D. 1950–1987 and 1988–2010) because a previous work suggests that a NPGO-related climate transition occurred in the late 1980s (Yeh et al. 2011). Our analysis reveals that significant correlations are found for the period from A.D. 1950–1987, and the highest correlation exists for 5–30-year variability of +MJ NPGO index ($r = 0.69$, d$f = 12$, $p = 0.001$; Table 2). However, there is no significant correlation between tree-ring δ^{18}O and the NPGO index during A.D. 1988–2010 (Table 2). These results suggest that tree-ring δ^{18}O in northeast Japan has a potential linkage with NPGO index from winter to early summer of the following year before the North Pacific climate transition in the late 1980s, especially on decadal timescales.

To better understand the relationship between early-summer precipitation in northeast Japan and the North Pacific climate pattern, we also compared inverted MJ precipitation in Sendai (because tree-ring δ^{18}O is negatively correlated with observed MJ precipitation as shown in Fig. 2a) to the NPGO index (Di Lorenzo et al. 2008) from A.D. 1950 to 2010. Similar time-lagged correlation analyses indicate that the highest correlation exists for +MJ NPGO index ($r = 0.24$, $p < 0.1$, $N = 61$) (Additional file 4: Table S1). Spectral analyses of both the raw and filtered tree-ring δ^{18}O and NPGO index showed similar variations on both multiyear and decadal timescales (Additional file 2: Figure S2, Additional file 3: Figure S3). To further examine the relationship between the actual early-summer precipitation

Table 1 Correlation coefficients between tree-ring δ^{18}O and two indices (NPGO and PDO)

Correlation	MJ	JA	SO	ND	+JF	+MA	+MJ
NPGO	0.20	0.23	0.18	0.15	0.28*	0.23	0.26*
PDO	− 0.12	− 0.06	− 0.10	− 0.10	0.01	0.01	− 0.03

* 0.05 significant level

+ means the following year, and analysis period is from A.D. 1950 to 2010

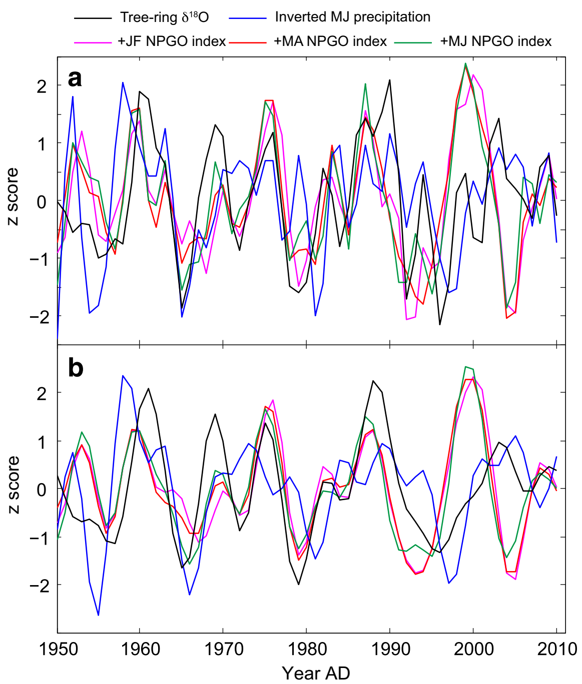

Fig. 5 **a** 3–30-year variability of tree-ring $\delta^{18}O$ (black line), inverted MJ precipitation in Sendai (blue line), +JF (magenta line), +MA (red line), and +MJ (green line) NPGO index. **b** Same as **a**, except for 5–30-year variability

Table 2 Correlation coefficients between tree-ring $\delta^{18}O$ and NPGO index after band-pass filtration

Correlation	+JF	+MA	+MJ
3–30 years band-pass (A.D. 1950–2010)	0.37	0.35	0.39
5–30 years band-pass (A.D. 1950–2010)	0.36	0.40	0.44
3–30 years band-pass (A.D. 1950–1987)	0.55*	0.61**	0.60**
5–30 years band-pass (A.D. 1950–1987)	0.54*	0.67*	0.69**
3–30 years band-pass (A.D. 1988–2010)	0.22	0.11	0.15
5–30 years band-pass (A.D. 1988–2010)	0.20	0.17	0.17

* 0.05 significant level using estimates of degree of freedom

** 0.01 significant level using estimates of degree of freedom

+ means the following year

and NPGO index on decadal time scales, we also performed the same comparison using band-pass filters. Considering the effective number of degree of freedom, 3–30-year variation of the inverted MJ precipitation significantly correlates with that of NPGO index from spring to early summer of the following year during only A.D. 1950–1987 (Table 3 and Fig. 5). These results suggest that the relationship between tree-ring $\delta^{18}O$ and the NPGO index from +MA to +MJ is consistent with that of observed early-summer precipitation on 3–30-year variability. Our results also propose that there are stronger relationships between the tree-ring $\delta^{18}O$ and the NPGO indices than between the MJ precipitation and the NPGO indices. Tree-ring cellulose $\delta^{18}O$ is theoretically controlled by the oxygen isotopes of precipitation and relative humidity (Roden et al. 2000; McCarroll and Loader 2004; Sternberg 2009; Managave et al. 2010). This rainfall $\delta^{18}O$ is influenced by not only precipitation amount but also moisture source change in the Japanese region (e.g., Kurita et al. 2015). The northeasterly "Yamase" winds sometimes affect the early summer weather in northeast Japan. Tree-ring cellulose $\delta^{18}O$ in northeast Japan may record this atmospheric circulation change. This may relate to the higher correlation coefficients than those of precipitation, but further work is needed to confirm this interpretation.

Table 3 Correlation coefficients between inverted MJ precipitation in Sendai and NPGO index after band-pass filtration

Correlation	+JF	+MA	+MJ
3–30 years band-pass (A.D. 1950–2010)	0.13	0.17	0.28
5–30 years band-pass (A.D. 1950–2010)	0.05	0.07	0.15
3–30 years band-pass (A.D. 1950–1987)	0.35	0.51*	0.56*
5–30 years band-pass (A.D. 1950–1987)	0.33	0.42	0.45
3–30 years band-pass (A.D. 1988–2010)	− 0.19	− 0.35	− 0.23
5–30 year band-pass (A.D. 1988–2010)	− 0.29	− 0.36	− 0.26

* 0.05 significant level using estimates of degree of freedom

+ means the following year using estimates of degree of freedom

To examine the relationship between our record and NPGO including prior to A.D. 1950, we examined +MA and +MJ mean global SST anomalies for six events of negative tree-ring $\delta^{18}O$ values, because the NPGO index values are not available prior to A.D. 1950 (Di Lorenzo et al. 2008). We denote 6 years (A.D. 1938, 1947, 1954, 1956, 1966 and 1981) based on tree-ring $\delta^{18}O$ (MJ precipitation in Sendai) indicating relatively low (high) values from the series mean (Fig. 3a). +MA and +MJ mean SST anomalies indicate that positive anomalies appear in the central North Pacific (Fig. 6a, b). The negative anomalies in the eastern North Pacific were only found in +MA mean SST anomalies (Fig. 6a). These dipole SST anomaly patterns may relate to the NPGO. We also performed the same analysis for six events of positive tree-ring $\delta^{18}O$ values (A.D. 1933, 1940, 1942, 1963, 1975, and 1987). +MA mean SST anomalies in the North Pacific had the opposite SST pattern (Fig. 6c), but these characteristics were not clear in +MJ mean SST anomalies (Fig. 6d). These results support the interpretation that our tree-ring $\delta^{18}O$ variability is related to the NPGO in spring of the following year prior to the late 1980s.

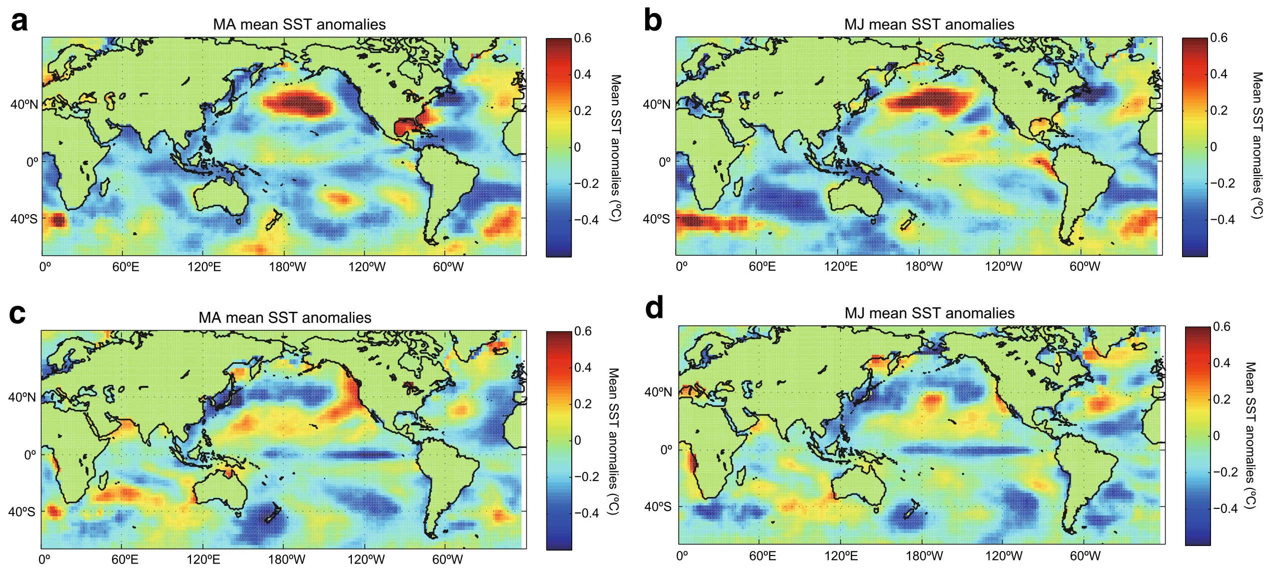

Fig. 6 **a** +MA and **b** +MJ mean SST anomalies for six negative tree-ring cellulose events (A.D. 1938, 1947, 1954, 1956, 1966 and 1981). **c** +MA and **d** +MJ mean SST anomalies for six positive tree-ring cellulose events (A.D. 1933, 1940, 1942, 1963, 1975, and 1987). Datasets were from ERSST (Smith et al. 2008), and these anomalies were calculated from the difference between SST in these years and the SST average during A.D. 1927–2010

Changes in sea-level pressure pattern

To explain the physical process linking our tree-ring δ^{18}O with the NPGO, we examined the MJ mean SLP pattern for four events of negative tree-ring δ^{18}O values (A.D. 1954, 1956, 1966 and 1981). Here spatial SLP datasets (Kalnay et al. 1996) were normalized to zero mean and one standard deviation during A.D. 1948–2010. This analysis showed that the MJ mean SLP anomalies were characterized by a dipole pattern in the western North Pacific (Fig. 7a). We also performed the same analysis for three events of positive tree-ring δ^{18}O values (A.D. 1963, 1975, and 1987). This indicated that the opposite dipole pattern appeared in the North Pacific (Fig. 7b). Previous work suggests these SLP patterns may relate to the NPO (Rogers 1981), and that this meridional pressure pattern may relate to the mean position of rain front and affect the early-summer hydrological climate in northeast Japan. To examine these SLP patterns including prior to A.D. 1950, the same analyses were performed using both the 20th century Reanalysis V2 of NOAA ESRL (Compo et al. 2011) and the ERA-20C datasets (Poli et al. 2016) from A.D. 1927 to 2010 (Additional file 5: Figure S4). In the analysis for six events of negative tree-ring δ^{18}O values (A.D. 1938, 1947, 1954, 1956, 1966, and 1981), the MJ mean SLP patterns in the Sea of Okhotsk had similar positive anomalies in Fig. 7a (Additional file 5: Figure S4a, b). The same analysis for six events of positive tree-ring δ^{18}O values (A.D. 1933, 1940, 1942, 1963, 1975, and 1987) also suggested that the SLP anomalies in the Sea of Okhotsk had negative trend (Additional file 5: Figure S4c, d), but the dipole pattern in the western North Pacific was unclear in these analyses (Additional file 5: Figure S4). This may indicate the weak relationship between our tree-ring δ^{18}O and the SLP pattern prior to A.D. 1950.

Meteorological data show a possible relationship between the WNPSM and the NPGO (Zhang and Luo 2016), with the relationship between the WNPSM and SLP in the North Pacific being built through the meridional wave train pattern in summer, resulting in a NPO pattern. The NPO forces sea-surface wind stress, causing then the NPGO-pattern SST anomaly to appear in the North Pacific during the following spring. Our analysis between tree-ring δ^{18}O in northeastern Japan and the NPGO indicate significant correlations with the +MA and +MJ NPGO index before the North Pacific climate transition in the late 1980s. Analyses using global SLP datasets also show that summer spatial SLP anomalies were a NPO-like pattern in A.D. 1938 and 1981. These are similar to the previous proposal of Zhang and Luo (2016), indicating that NPGO can be reconstructed by measuring the tree-ring δ^{18}O in northeastern Japan prior to late 1980s. Previous studies reported that the regime shift of meridional circulation occurred in the North Pacific in the late 1980s (e.g., Xiao et al. 2012; Kim et al. 2015). This meridional circulation change may relate to the weak relationship between our tree-ring δ^{18}O and the NPGO after the late 1980s, but further investigations are needed to confirm this interpretation.

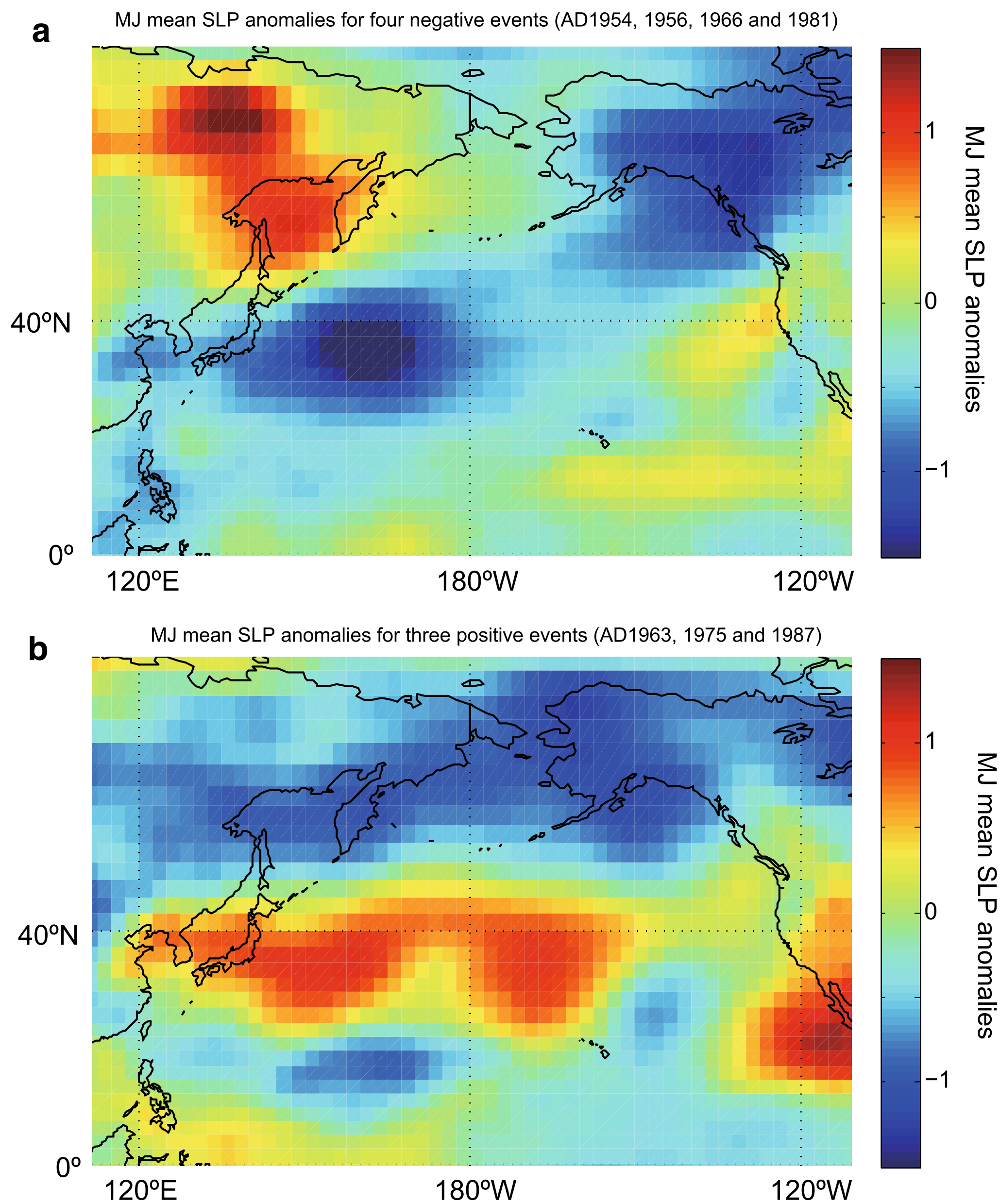

Fig. 7 **a** MJ mean SLP anomalies for four negative tree-ring cellulose events (A.D. 1954, 1956, 1966 and 1981). **b** MJ mean SLP anomalies for three positive tree-ring cellulose events (A.D. 1963, 1975, and 1987). Datasets were from NCEP/NCAR reanalysis 1 (Kalnay et al. 1996). These anomalies were normalized to zero mean and one standard deviation during A.D. 1948–2010

Conclusions

This study has examined the relation between tree-ring $\delta^{18}O$ variability in northeastern Japan and the NPGO. Our analyses reveal that this tree-ring $\delta^{18}O$ signal is controlled by the early-summer hydrological climate change, except for the long-term relative humidity variation. Time-lagged temporal-domain comparisons to the NPGO index indicate that our hydroclimate reconstruction data relate to the +MA and +MJ NPGO before the North Pacific climate transition in the late 1980s, and this relationship is strong on decadal timescales. These results are consistent with the observed early-summer precipitation. Spatial spring and early-summer SST anomalies indicate NPGO-like patterns in the following year. Spatial early-summer SLP anomalies show dipole patterns in the western North Pacific, which may relate to the NPO. These time-lagged responses are consistent with previous works. Our results point towards a potential linkage between tree-ring δ^{18}O variability in northeastern Japan and the NPGO, but more work is needed to understand its exact nature and identify mechanisms.

Additional files

Additional file 1: Figure S1. Same as Fig. 2, except for (a) monthly mean precipitation, (b) three-month average precipitation, (c) four-month average precipitation, (d) monthly mean relative humidity (RH), (e) three-month average RH, (f) four-month average RH, (g) two-month average temperature, (h) three-month average temperature, and (i) four-month average temperature.

Additional file 2: Figure S2. Results of MTM analysis for (a) tree-ring δ^{18}O, (b) following year January-February (+JF), (c) following year March-April (+MA), and (d) following year May-June (+MJ) NPGO index. Analysis period is from AD 1950 to 2010. Red solid lines indicate 95 and 99% significant level. Black dot lines correspond to 3-, 5- and 30-year cycles.

Additional file 3: Figure S3. Wavelet coherence between the tree-ring δ^{18}O and (a) +JF, (b) +MA, and (c) +MJ NPGO index. Black contour indicates the 95% significant level, and white shade means the cone of influence.

Additional file 4: Table S1. Correlation coefficients between inverted MJ precipitation in Sendai and NPGO index.

Additional file 5: Figure S4. (a) MJ mean SLP anomalies for six events of negative tree-ring δ^{18}O values (AD 1938, 1947, 1954, 1956, 1966 and 1981) using the 20th century Reanalysis V2 of NOAA ESRL (Compo et al. 2011). (b) Same as Fig. S4a, except for using the ERA-20C datasets (Poli et al. 2016). (c) MJ mean SLP anomalies for six events of positive tree-ring δ^{18}O values (AD 1933, 1940, 1942, 1963, 1975 and 1987) using the 20th century Reanalysis V2 of NOAA ESRL (Compo et al. 2011). (d) Same as Fig. S4c, except for using the ERA-20C datasets (Poli et al. 2016). These anomalies were normalized to zero mean and one standard deviation during AD 1927–2010.

Abbreviations
EASM: East Asian summer monsoon; EOF: empirical orthogonal function; JF: January–February; KOE: Kuroshio–Oyashio Extension; MA: March–April; MJ: May–June; MTM: multitaper method; NPGO: North Pacific Gyre Oscillation; NPO: North Pacific Oscillation; PDO: Pacific Decadal Oscillation; SLP: sea-level pressure; SSH: sea-surface height; SST: sea-surface temperature; WNPSM: Western North Pacific summer monsoon.

Authors' contributions
WS: Sampling, measurement of cellulose δ^{18}O, analysis, interpretation, and writing the manuscript. HM and SO: Analysis, interpretation, and help in writing the manuscript. YY: Sampling, interpretation, and supervising this study. TA and TN: Measurement of cellulose δ^{18}O. All authors read and approved the final manuscript.

Author details
[1] Humanities and Sciences, Musashino Art University, 1-736 Ogawa-cho, Kodaira, Tokyo 187-8505, Japan. [2] Faculty of Life and Environmental Sciences, University of Tsukuba, 1-1-1 Ten-nodai, Tsukuba, Ibaraki 305-8572, Japan. [3] Atmosphere and Ocean Research Institute, The University of Tokyo, 5-1-5 Kashiwanoha, Kashiwa, Chiba 277-8564, Japan. [4] Department of Earth and Planetary Science, Graduate School of Science, The University of Tokyo, 7-3-1 Hongo, Tokyo 113-0033, Japan. [5] Department of Biogeochemistry, Japan Agency for Marine-Earth Science and Technology (JAMSTEC), 2-15 Natsushima-cho, Yokosuka, Kanagawa 237-0061, Japan. [6] Faculty of International Resource Science, Akita University, 1-1 Tegata Gakuen-machi, Akita 010-8502, Japan. [7] Research Institute for Humanity and Nature (RIHN), 457-4 Motoyama, Kamigamo, Kita-ku, Kyoto 603-8047, Japan.

Acknowledgements
The authors would like to express their appreciations to Y. Ueno of Tokyo Institute of Technology for providing us with his laboratory space for our measurements of tree-ring cellulose δ^{18}O. We also would like to express our gratitude to Kashima shrine and A. Saito of Kami-machi Board of Education for providing our tree sample. The authors also thank two anonymous reviewers for their comments and suggestions. This investigation was supported by the Japan Society for the Promotion of Science (JSPS) KAKENHI program (Grant Numbers JP15H05816, JP25287051, JP25247082, JP26247085, JP15KK0151, and JP16K05571). This research was also funded by the program for JSPS Research Fellows DC1 (JP12J10623).

Competing interests
The authors declare that they have no competing interests.

Availability of data and materials
Tree-ring cellulose δ^{18}O data may be obtained from WS (sakashita.wataru.fu@u.tsukuba.ac.jp).

Consent for publication
All authors agree for this publication.

Ethics approval and consent to participate
We consent to participate and have no competing interests.

Funding
This investigation was supported by the Japan Society for the Promotion of Science (JSPS) KAKENHI program (Grant Numbers JP15H05816, JP25287051, JP25247082, JP26247085, JP15KK0151, and JP16K05571). This research was also funded by the program for JSPS Research Fellows DC1 (JP12J10623).

Publisher's Note
Springer Nature remains neutral with regard to jurisdictional claims in published maps and institutional affiliations.

Received: 12 July 2017 Accepted: 5 December 2017
Published online: 12 December 2017

References
Bond NA, Harrison DE (2000) The Pacific decadal oscillation, air-sea interaction and central north Pacific winter atmospheric regimes. Geophys Res Lett 27:731–734. https://doi.org/10.1029/1999GL010847
Ceballos LI, Di Lorenzo E, Hoyos CD et al (2009) North Pacific gyre oscillation synchronizes climate fluctuations in the eastern and western boundary systems. J Clim 22:5163–5174. https://doi.org/10.1175/2009JCLI2848.1
Compo GP, Whitaker JS, Sardeshmukh PD et al (2011) The twentieth century reanalysis project. Q J R Meteorol Soc 137:1–28. https://doi.org/10.1002/qj.776
Craig H, Gordon LI (1965) Deuterium and oxygen 18 variations in the ocean and the marine atmosphere. Consiglio nazionale delle richerche, Laboratorio de geologia nucleare, Pisa
Dansgaard W (1964) Stable isotopes in precipitation. Tellus 16:436–468
D'Arrigo R, Wilson R (2006) On the Asian expression of the PDO. Int J Climatol 26:1607–1617. https://doi.org/10.1002/joc.1326
Di Lorenzo E, Schneider N, Cobb KM et al (2008) North Pacific Gyre Oscillation links ocean climate and ecosystem change. Geophys Res Lett 35:2–7. https://doi.org/10.1029/2007GL032838
Di Lorenzo E, Cobb KM, Furtado JC et al (2010) Central Pacific El Niño and decadal climate change in the North Pacific Ocean. Nat Geosci 3:762–765. https://doi.org/10.1038/ngeo984
England MH, McGregor S, Spence P et al (2014) Recent intensification of wind-driven circulation in the Pacific and the ongoing warming hiatus. Nat Clim Chang 4:222–227. https://doi.org/10.1038/NCLIMATE2106
Felis T, Suzuki A, Kuhnert H et al (2010) Pacific decadal oscillation documented in a coral record of North Pacific winter temperature since 1873. Geophys Res Lett 37:2000–2005. https://doi.org/10.1029/2010GL043572

Ghil M (2002) Advanced spectral methods for climatic time series. Rev Geophys 40:1003. https://doi.org/10.1029/2000RG000092
Grinsted A, Moore JC, Jevrejeva S (2004) Application of the cross wavelet transform and wavelet coherence to geophysical time series. Nonlinear Process Geophys 11:561–566. https://doi.org/10.5194/npg-11-561-2004
Kagawa A, Sano M, Nakatsuka T et al (2015) An optimized method for stable isotope analysis of tree rings by extracting cellulose directly from cross-sectional laths. Chem Geol 393–394:16–25. https://doi.org/10.1016/j.chemgeo.2014.11.019
Kalnay E, Kanamitsu M, Kistler R et al (1996) The NCEP/NCAR 40-year reanalysis project. Bull Am Meteorol Soc 77:437–471
Kim YH, Kim MK, Lau WKM et al (2015) Possible mechanism of abrupt jump in winter surface air temperature in the late 1980s over the Northern Hemisphere. J Geophys Res Atmos 120:12474–12485. https://doi.org/10.1002/2015JD023864
Kurita N, Fujiyoshi Y, Nakayama T et al (2015) East Asian Monsoon controls on the inter-annual variability in precipitation isotope ratio in Japan. Clim Past 11:339–353. https://doi.org/10.5194/cp-11-339-2015
Li Z, Nakatsuka T, Sano M (2015) Tree-ring cellulose $\delta^{18}O$ variability in pine and oak and its potential to reconstruct precipitation and relative humidity in central Japan. Geochem J 49:125–137. https://doi.org/10.2343/geochemj.2.0336
Managave SR, Sheshshayee MS, Borgaonkar HP, Ramesh R (2010) Past break-monsoon conditions detectable by high resolution intra-annual δ 18 O analysis of teak rings. Geophys Res Lett 37:L05702. https://doi.org/10.1029/2009GL041172
Mantua NJ, Hare SR, Zhang Y, Wallace JM, Francis RC (1997) A Pacific interdecadal climate oscillation with impacts on salmon production. Bull Am Meteorol Soc 78:1069–1079
McCarroll D, Loader NJ (2004) Stable isotopes in tree rings. Quat Sci Rev 23:771–801. https://doi.org/10.1016/j.quascirev.2003.06.017
Nurhati IS, Cobb KM, Di Lorenzo E (2011) Decadal-scale SST and salinity variations in the central tropical pacific: signatures of natural and anthropogenic climate change. J Clim 24:3294–3308. https://doi.org/10.1175/2011JCLI3852.1
Poli P, Hersbach H, Dee DP et al (2016) ERA-20C: an atmospheric reanalysis of the twentieth century. J Clim 29:4083–4097. https://doi.org/10.1175/JCLI-D-15-0556.1
Rafter PA, Sanchez SC, Ferguson J et al (2017) Eastern tropical North Pacific coral radiocarbon reveals North Pacific Gyre Oscillation (NPGO) variability. Quat Sci Rev 160:108–115. https://doi.org/10.1016/j.quascirev.2017.02.002
Roden JS, Lin G, Ehleringer JR (2000) A mechanistic model for interpretation of hydrogen and oxygen isotope ratios in tree-ring cellulose. Geochim Cosmochim Acta 64:21–35. https://doi.org/10.1016/S0016-7037(99)00195-7
Rogers JC (1981) The North Pacific Oscillation. J Climatol 1:39–57. https://doi.org/10.1002/joc.3370010106
Sakashita W, Yokoyama Y, Miyahara H et al (2016) Relationship between early summer precipitation in Japan and the El Niño-Southern and Pacific Decadal Oscillations over the past 400 years. Quat Int 397:300–306. https://doi.org/10.1016/j.quaint.2015.05.054
Sakashita W, Miyahara H, Yokoyama Y et al (2017) Hydroclimate reconstruction in central Japan over the past four centuries from tree-ring cellulose δ 18 O. Quat Int. https://doi.org/10.1016/j.quaint.2017.06.020
Sano M, Xu C, Nakatsuka T (2012) A 300-year Vietnam hydroclimate and ENSO variability record reconstructed from tree ring δ 18 O. J Geophys Res Atmos 117:D12115. https://doi.org/10.1029/2012JD017749
Sato T, Shiraiwa T, Greve R et al (2014) Accumulation reconstruction and water isotope analysis for 1736–1997 of an ice core from the Ushkovsky volcano, Kamchatka, and their relationships to North Pacific climate records. Clim Past 10:393–404. https://doi.org/10.5194/cp-10-393-2014
Shen C, Wang WC, Gong W, Hao Z (2006) A Pacific Decadal Oscillation record since 1470 AD reconstructed from proxy data of summer rainfall over eastern China. Geophys Res Lett 33:L03702. https://doi.org/10.1029/2005GL024804
Smith TM, Reynolds RW, Peterson TC, Lawrimore J (2008) Improvements to NOAA's historical merged land-ocean surface temperature analysis (1880–2006). J Clim 21:2283–2296. https://doi.org/10.1175/2007JCLI2100.1
Sternberg LSL (2009) Oxygen stable isotope ratios of tree-ring cellulose: the next phase of understanding. New Phytol 181:553–562
Xiao D, Li J, Zhao P (2012) Four-dimensional structures and physical process of the decadal abrupt changes of the northern extratropical ocean-atmosphere system in the 1980s. Int J Climatol 32:983–994. https://doi.org/10.1002/joc.2326
Xu C, Sano M, Nakatsuka T (2011) Tree ring cellulose δ 18 O of Fokienia hodginsii in northern Laos: a promising proxy to reconstruct ENSO? J Geophys Res Atmos 116:D24109. https://doi.org/10.1029/2011JD016694
Yamaguchi YT, Yokoyama Y, Miyahara H et al (2010) Synchronized Northern Hemisphere climate change and solar magnetic cycles during the Maunder Minimum. Proc Natl Acad Sci USA 107:20697–20702. https://doi.org/10.1073/pnas.1000113107
Ye X, Zhang W, Luo M (2016) The North Pacific Gyre Oscillation and East Asian summer precipitation. Atmos Sci Lett 17:531–537. https://doi.org/10.1002/asl.688
Yeh SW, Kang YJ, Noh Y, Miller AJ (2011) The North Pacific climate transitions of the winters of 1976/77 and 1988/89. J Clim 24:1170–1183. https://doi.org/10.1175/2010JCLI3325.1
Yokoyama Y, Suzuki A, Siringan F et al (2011) Mid-Holocene palaeoceanography of the northern South China Sea using coupled fossil-modern coral and atmosphere-ocean GCM model. Geophys Res Lett 38:3. https://doi.org/10.1029/2010gl044231
Zhang W, Luo M (2016) A possible linkage of the western North Pacific summer monsoon with the North Pacific Gyre Oscillation. Atmos Sci Lett 17:437–445. https://doi.org/10.1002/asl.676
Zhang Y, Wallace JM, Battisti DS (1997) ENSO-like interdecadal variability: 1900–93. J Clim 10:1004–1020. https://doi.org/10.1175/1520-0442(1997)010<1004:ELIV>2.0.CO;2